inorganics

MDPI

Article

Ammonothermal Synthesis and Crystal Structures of Diamminetriamidodizinc Chloride $[Zn_2(NH_3)_2(NH_2)_3]Cl$ and Diamminemonoamidozinc Bromide $[Zn(NH_3)_2(NH_2)]Br$

Theresia M. M. Richter [1], Sabine Strobel [1], Nicolas S. A. Alt [2], Eberhard Schlücker [2] and Rainer Niewa [1,*]

[1] Institute of Inorganic Chemistry, Universität Stuttgart, Pfaffenwaldring 55, 70569 Stuttgart, Germany; richter.theresia@yahoo.de (T.M.M.R.); sabine.strobel@iac.uni-stuttgart.de (S.S.)

[2] Institute of Process Machinery and Systems Engineering, University of Erlangen-Nuremberg, Cauerstraße 4, 91058 Erlangen, Germany; nicolas.alt@hswt.de (N.S.A.A.); sl@ipat.uni-erlangen.de (E.S.)

* Correspondence: rainer.niewa@iac.uni-stuttgart.de; Tel.: +49-711-6856-4217

Academic Editors: Helmut Cölfen and Duncan H. Gregory
Received: 7 November 2016; Accepted: 6 December 2016; Published: 9 December 2016

Abstract: The treatment of excess zinc in the presence of ammonium chloride under ammonothermal conditions of 873 K and 97 MPa leads to diamminetriamidodizinc chloride $[Zn_2(NH_3)_2(NH_2)_3]Cl$ with a two-dimensionally μ-amido-interconnected substructure. Similar reaction conditions using ammonium bromide instead of the chloride (773 K, 230 MPa) result in diamminemonoamidozinc bromide $[Zn(NH_3)_2(NH_2)]Br$ with one-dimensional infinite μ-amido-bridged chains. Both compounds were obtained as colorless, very moisture sensitive crystals. Crystal structures and hydrogen bond schemes are analyzed. Raman spectroscopic data of the chloride are reported.

Keywords: ammonothermal synthesis; amides; ammoniates; zinc

1. Introduction

Synthesis of high-quality nitride materials presents a challenge for various applications. In particular, semiconductor nitride materials are currently the focus of crystal growth, one example being GaN wafers as superior substrates for high-performance blue and white LEDs [1]. A promising synthesis and crystal growth technique for such materials is the ammonothermal method, utilizing supercritical ammonia under either ammonoacidic or ammonobasic conditions. However, a number of unresolved issues remain, like the fundamental understanding of the chemistry of dissolution, materials transport and recrystallization processes. Additionally, the technique may not only provide superior GaN crystals, but further interesting nitride materials.

Recently, we have focused on the ammonothermal zinc nitride synthesis. In this respect, we have presented the ammonothermal synthesis and characterization of $Zn(NH_3)_3F_2$ and $Zn(NH_3)_2F_2$, which show five-fold coordination at Zn [2]. In contrast, the few further examples of ammoniates of zinc halides exclusively exhibit the tetrahedral environment of Zn, namely in $[Zn(NH_3)_2Cl_2]$, $[Zn(NH_3)_2Br_2]$ [3], $[Zn(NH_3)_4]Br_2$ and $[Zn(NH_3)_4]I_2$ [4], all obtained from reaction of either aqueous solutions or of the solid zinc halides with ammonia at ambient pressure. With $[Zn_2(NH_3)_2(NH_2)_3]Cl$ and $[Zn(NH_3)_2(NH_2)]Br$, we present two ammineamidozinc halides, synthesized from nominally ammonoacidic conditions, which additionally show increased condensation within their cationic substructures. The formation of these compounds from supercritical ammonia may indicate their role as intermediates in a conceivable ammonothermal synthesis and crystal growth of the interesting

semiconductor material Zn_3N_2 analogously to the already commercially available ammonothermally grown GaN crystals [1].

2. Results and Discussion

We present the synthesis of $[Zn_2(NH_3)_2(NH_2)_3]Cl$ and $[Zn(NH_3)_2(NH_2)]Br$, two ammoniates of zinc halide amides, both with tetrahedral coordination by ammonia and amide ligands at the Zn central atom. Similar simultaneous coordination by amide ions and ammonia molecules was previously reported in, for example, $KNH_2 \cdot 2NH_3$ [5], or more relevant for the discussion, $[Cr_2(NH_2)_3(NH_3)_6]I_2$ [6] and $InF_2(NH_2)(NH_3)$ [7], both with octahedral coordination at the metal atom and obtained from the respective halides under ammonothermal conditions.

Both title compounds were obtained in the colder zone of the autoclave, while additional $Zn(NH_2)_2$ was observed in the hot zone. According to literature, $Zn(NH_2)_2$ is insoluble in liquid ammonia at ambient conditions [8]; however, we have frequently observed that Zn reacts under various ammonoacidic as well as ammonobasic conditions to form the diamide and crystallizes in the colder zone of the autoclave in large crystals, indicating the ammonoamphoteric character of Zn and an enhanced solubility of the binary amide at elevated temperatures and pressures. However, it is apparently possible to adjust the solubility, respectively its temperature dependence, by the addition of halide ions and thus favor the formation of the supposedly less soluble title compounds in the zone with lower temperature. The deposition at the hotter or colder zone in the reaction vessel is usually dictated by the temperature dependence of the solubility. This temperature dependence can fundamentally change with the type of mineralizer and therefore with the nature of the dissolved species, as is well known, for example, for the ammonothermal synthesis of GaN [1].

The underlying thermodynamics governing these processes follow very similar principles to those that are well established for the so-called Chemical Vapor Transport [9].

It is interesting to note that we were only able to synthesize the title compounds in the presence of platinum used as liner material to minimize contact of the solution with the autoclave wall and thus minimize corrosion, known to be severe in ammonoacidic solutions at elevated temperatures [10]. A catalytic action of both NH_4Cl and Pt, for example, for the formation of alkali- and alkaline-earth metal amides from liquid ammonia is well established [11].

2.1. Crystal Structure Description

$[Zn_2(NH_3)_2(NH_2)_3]Cl$ crystallizes in the chiral space group $P2_12_12$ with two formula units in the unit cell. A Flack parameter close to $\frac{1}{2}$ indicates the presence of a racemic inversion twin. Table 1 gives further selected information on the crystal structure and its determination. Table 2 presents positional parameters and Table A1 anisotropic displacement parameters. In the crystal structure, the ammonia molecules, the amide and the chloride ions together form the motif of a hexagonal closed packing with stacking of hexagonal layers along [100]. In addition, 1/6 of the tetrahedral voids exclusively built by ammonia molecules and amide groups are occupied by Zn. These tetrahedra are linked via amide vertices to layers ${}^2_\infty\left[Zn(NH_3)(NH_2)_{3/2}{}^{1/2+}\right]$ orientated within the a/b plane (Figure 1). As may be expected, the distances Zn–N to the amide groups with 199.1(5) pm and 201.2(6) pm are significantly shorter as compared to the distance to the NH_3 ligand (213.5(7) pm). Similar distance relations were earlier observed, e.g., in $KNH_2 \cdot 2NH_3$ [5] or $[Cr_2(NH_2)_3(NH_3)_6]I_3$ [6]. Angles around Zn are in the range of 101.8° to 116.4°, thus close to the ideal tetrahedral angle. Further selected distances and angles are summarized in Table 3.

The arrangement of tetrahedra within the layer ${}^2_\infty\left[Zn(NH_3)(NH_2)_{3/2}{}^{1/2+}\right]$ is reminiscent of the very similar interconnection within the structure of binary $Zn(NH_2)_2$, where six tetrahedra are condensed to rings, however, interconnected within a three-dimensional framework. According to the nomenclature after Liebau, developed to classify oxosilicate structures, ${}^2_\infty\left[Zn(NH_3)(NH_2)_{3/2}{}^{1/2+}\right]$ represents an unbranched *vierer* single-layer with a molar ratio n(Zn):n(N) of 2:5 [12].

Table 1. Selected crystallographic data and information for the structure determination of $[Zn_2(NH_3)_2(NH_2)_3]Cl$ and $[Zn(NH_3)_2(NH_2)]Br$.

Formula	$[Zn_2(NH_3)_2(NH_2)_3]Cl$	$[Zn(NH_3)_2(NH_2)]Br$ [a]
Crystal system	orthorhombic	monoclinic
Space group	$P2_12_12$	$P2_1/n$
a/pm	577.15(4)	760.55(4)
b/pm	1023.59(6)	597.72(4)
c/pm	654.56(4)	1257.22(8)
β/deg.	-	93.475(4)
$V/10^6$ pm^3	386.69(5)	570.48(6)
X-ray density ρ_{XRD}/g/cm^3	2.13	2.28
Z	2	4
T	298 K	100 K
Radiation	Mo-$K\alpha$	Mo-$K\alpha$
$F(000)$	496	376
Range $h/k/l$	±4/−13–14/−21–22	±8/±11/−17–16
θ_{max}/deg.	53.9	55.0
Absorption coefficient/mm^{-1}	12.93	11.17
Reflect. meas./indep.	844/533	1298/751
R_{int}/R_σ	0.030/0.038	0.030/0.036
$R_1(\lvert F_o \rvert \geq 4\sigma(F_o))$	0.038	0.034
R_1/wR_2/GooF(all refl.)	0.044/0.098/1.021	0.045/0.086/1.047
Parameters	58	71
Restraints	6	8
Extinction coefficient	0.017(6)	0.003(1)
Flack x	0.49(4)	-
Residual e$^-$-density/10^{-6}·pm^{-3}	1.19/−0.54	1.23/−1.13

[a] Refined as twin by partial merohedry.

Table 2. Positional and isotropic displacement parameters U_{iso} (10^4 pm^2) for $[Zn_2(NH_3)_2(NH_2)_3]Cl$.

Atom	Site	x	y	z	U_{iso}
Zn	4c	0.1009(1)	0.33764(8)	0.5374(1)	0.0231(3)
Cl	2a	1/2	1/2	0.0434(5)	0.0247(5)
N(1)	4c	0.449(1)	0.3291(7)	0.553(1)	0.028(1)
H(1A)	4c	0.35(2)	0.248(8)	0.67(1)	$1.2U_{iso}$(N(1))
H(1B)	4c	0.50(2)	0.354(1)	0.67(1)	$1.2U_{iso}$(N(1))
N(2)	4c	0.007(1)	0.3377(8)	0.853(1)	0.032(1)
H(2A)	4c	0.00(2)	0.259(5)	0.91(1)	$1.2U_{iso}$(N(2))
H(2B)	4c	0.09(2)	0.36(1)	0.96(1)	$1.2U_{iso}$(N(2))
H(2C)	4c	0.41(2)	0.118(9)	0.08(1)	$1.2U_{iso}$(N(2))
N(3)	2b	0	1/2	0.395(2)	0.027(2)
H(3A)	4c	0.354(7)	0.01(1)	0.65(1)	$1.2U_{iso}$(N(3))

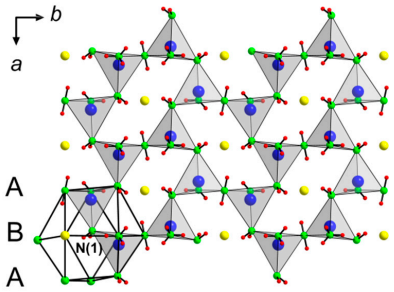

Figure 1. Section of the crystal structure of $[Zn_2(NH_3)_2(NH_2)_3]Cl$: Layers $^2_\infty\left[Zn(NH_3)(NH_2)_{3/2}\right]^{1/2+}$ built by occupation of tetrahedral voids exclusively formed by amide and ammonia molecules by Zn within the motif of an *hcp* of chloride (closed packed layers in stacking direction [100] are indicated by letters A and B), amide ions and ammonia molecules (**yellow** spheres: Cl, **green** spheres: N, **red** spheres: H, and **blue** spheres surrounded by **grey** tetrahedra: Zn). The *hcp* stacking motif is indicated by an anticuboctahedron and capital letters.

Table 3. Selected interatomic distances (pm) and angles (deg.) in the crystal structure of $[Zn_2(NH_3)_2(NH_2)_3]Cl$.

Bond		Distance	Occurence	Arrangement	Angle
Zn	–N(1)	200.9(7)		N(1)–Zn–N(1)	114.5(2)
Zn	–N(1)	201.2(6)		N(1)–Zn–N(2)	101.8(3)
Zn	–N(2)	213.5(7)		N(1)–Zn–N(2)	110.1(3)
Zn	–N(3)	199.1(5)		N(1)–Zn–N(3)	110.6(2)
				N(1)–Zn–N(3)	116.4(3)
				N(2)–Zn–N(3)	112.1(4)
N(1)	–H(1A)	88(3)		H(1A)–N(1)–H(1B)	107(9)
N(1)	–H(1B)	89(3)		Zn–N(1)–H(1A)	98(7)
				Zn–N(1)–H(1B)	102(7)
				Zn–N(1)–Zn	117.3(2)
N(2)	–H(2A)	88(3)		H(2A)–N(2)–H(2B)	87(9)
N(2)	–H(2B)	88(3)		H(2A)–N(2)–H(2C)	102(10)
N(2)	–H(2C)	89(3)		H(2B)–N(2)–H(2C)	70(8)
				Zn–N(2)–H(2A)	113(7)
				Zn–N(2)–H(2B)	130(7)
				Zn–N(2)–H(2C)	139(7)
N(3)	–H(3A)	90(3)	2x	H(3A)–N(3)–H(3A)	144(9)
				Zn–N(3)–H(3A)	105(7)
				Zn–N(3)–Zn	124.4(5)
∅N	–H	89			
∅Zn	–N	204			

Hydrogen atoms of the amide groups point towards the chloride ions located between the layers and form hydrogen bonds (Figure 2). Every chloride ion connects to twelve hydrogen atoms, where half of the hydrogen atoms belong to each neighboring layer. Table 4 summarizes donor–acceptor distances and angles.

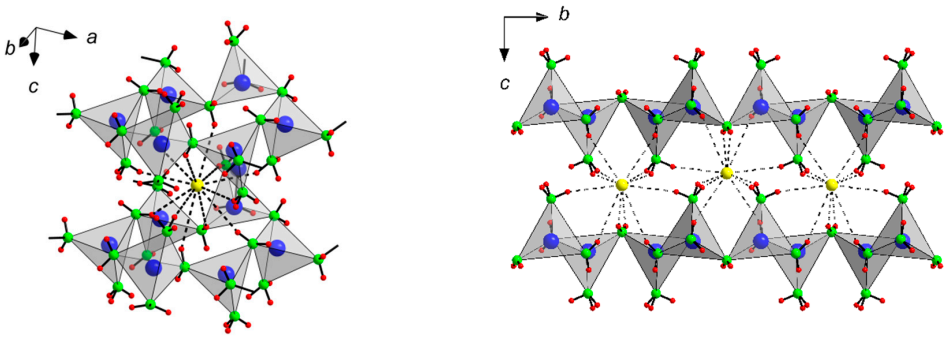

(**a**) (**b**)

Figure 2. Sections of the crystal structure of $[Zn_2(NH_3)_2(NH_2)_3]Cl$: (**a**) every chloride ion employs twelve H-bonds and (**b**) connects two adjacent layers $^2_\infty\left[Zn(NH_3)(NH_2)_{3/2}{}^{1/2+}\right]$ within the third dimension (**yellow** spheres: Cl, **green** spheres: N, **red** spheres: H, and **blue** spheres surrounded by **grey** tetrahedra: Zn).

Table 4. Donor–acceptor distances (pm) and angles (deg.) in $[Zn_2(NH_3)_2(NH_2)_3]Cl$.

Arrangement	*d*(N–H)	*d*(H . . . Cl)	<(NHCl)	*d*(N . . . Cl)
N(1)–H(1A) . . . Cl	88	304	143.0	378
N(1)–H(1B) . . . Cl	89	287	149.9	367
N(2)–H(2A) . . . Cl	89	267	163.2	352
N(2)–H(2B) . . . Cl	88	284	135.1	352
N(2)–H(2C) . . . Cl	89	274	161.7	359
N(3)–H(3A) . . . Cl	90	287	152.7	369

$[Zn(NH_3)_2(NH_2)]Br$ suffers from twinning by partial merohedry via two-fold rotation around the face diagonal [101] in space group $P12_1/n1$ setting. Due to application of the respective twin law, the reliability factors significantly drop (see the experimental part). Table 1 summarizes selected information for the final structure refinement, Table 5 gives positional parameters and Table A2 anisotropic displacement parameters.

Table 5. Positional and isotropic displacement parameters U_{iso} (10^4 pm^2) for $[Zn(NH_3)_2(NH_2)]Br$.

Atom	Site	x	y	z	U_{iso}
Br	4*e*	0.1858(4)	0.22474(7)	0.4382(4)	0.0214(3)
Zn	4*e*	0.1606(4)	0.1440(2)	0.7794(4)	0.0166(3)
N(1)	4*e*	0.163(3)	0.243(5)	0.9347(2)	0.021(2)
H(1A)	4*e*	0.054(9)	0.28(5)	0.95(2)	$1.5U_{iso}$(N(1))
H(1B)	4*e*	0.20(3)	0.14(2)	0.98(1)	$1.5U_{iso}$(N(1))
H(1C)	4*e*	0.23(2)	0.36(2)	0.94(1)	$1.5U_{iso}$(N(1))
N(2)	4*e*	0.419(4)	0.247(5)	0.206(2)	0.023(8)
H(2A)	4*e*	0.83(3)	0.22(2)	0.75(2)	$1.5U_{iso}$(N(2))
H(2B)	4*e*	0.89(3)	0.38(2)	0.67(1)	$1.5U_{iso}$(N(2))
H(2C)	4*e*	0.86(3)	0.13(2)	0.67(2)	$1.5U_{iso}$(N(2))
N(3)	4*e*	0.859(3)	0.190(1)	0.221(3)	0.015(3)
H(3A)	4*e*	0.95(1)	0.26(2)	0.257(8)	$1.2U_{iso}$(N(3))
H(3B)	4*e*	0.90(1)	0.20(2)	0.157(4)	$1.2U_{iso}$(N(3))

Very similar to $[Zn_2(NH_3)_2(NH_2)_3]Cl$, the ammonia molecules, amide and bromide ions in the crystal structure of $[Zn(NH_3)_2(NH_2)]Br$, form the motif of a hexagonal closed packing with stacking along [010] (Figure 3). According to the composition, only 1/8 of the tetrahedral voids exclusively formed by two ammonia molecules and two amide ions are occupied by Zn. As discussed above for the chloride, the distances to the terminal ammonia ligands with 204(3) pm and 211(3) pm are significantly longer than those to the bridging amide ligands with 198.4(8) pm and 200.2(8) pm. Angles around Zn with 104°–123.8° deviate little from to the ideal tetrahedral angle. Table 6 collects selected interatomic distances and angles. Vertex-sharing via amide ligands leads to $^1_\infty\left[Zn(NH_3)_2(NH_2)_{2/2}{}^+\right]$ zigzag chains running along [010]. According to the Liebau nomenclature, these chains are classified as unbranched *zweier* single-chains with molar ratio of *n*(Zn):*n*(N) = 1:3 [12]. Once again, these chains may be viewed as sections from the three-dimensional crystal structure of binary zinc amide, formally broken up by the addition of HBr.

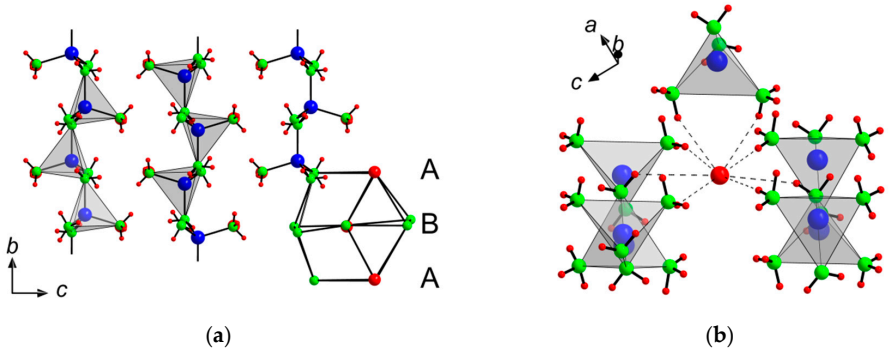

(**a**) (**b**)

Figure 3. Sections of the crystal structure of $[Zn(NH_3)_2(NH_2)]Br$: (**a**) infinite $^1_\infty\left[Zn(NH_3)_2(NH_2)_{2/2}{}^+\right]$ zigzag chains result from occupation of tetrahedral voids exclusively built by amide ions and ammonia molecules by Zn within the motif of an *hcp* formed by bromide and amide ions together with ammonia molecules (the *hcp* stacking motif is indicated by an anticuboctahedron and capital letters); (**b**) every bromide ion employs eight H-bonds and interconnects three chains (large **red** spheres: Cl, **green** spheres: N, small **red** spheres: H, and **blue** spheres surrounded by **grey** tetrahedra: Zn).

Table 6. Selected interatomic distances (pm) and angles (deg.) in the crystal structure of $[Zn(NH_3)_2(NH_2)]Br$.

Bond		Distance	Arrangement	Angle
Zn	–N(1)	204(3)	N(1)–Zn–N(2)	106.7(6)
Zn	–N(2)	211(3)	N(1)–Zn–N(3)	104(1)
Zn	–N(3)	198.4(8)	N(1)–Zn–N(3)	107(1)
Zn	–N(3)	200.2(8)	N(2)–Zn–N(3)	110(1)
			N(2)–Zn–N(3)	105(1)
N(1)	–H(1A)	91(7)	N(3)–Zn–N(3)	123.8(2)
N(1)	–H(1B)	89(3)	H(1A)–N(1)–H(1B)	103(10)
N(1)	–H(1C)	89(3)	H(1A)–N(1)–H(1C)	109(10)
			H(1B)–N(1)–H(1C)	110(10)
N(2)	–H(2A)	92(4)	Zn–N(1)–H(1A)	112(10)
N(2)	–H(2B)	90(4)	Zn–N(1)–H(1B)	116(10)
N(2)	–H(2C)	90(4)	Zn–N(1)–H(1C)	108(10)
			H(2A)–N(2)–H(2B)	112(10)
N(3)	–H(3A)	89(3)	H(2A)–N(2)–H(2C)	83(10)
N(3)	–H(3B)	89(3)	H(2B)–N(2)–H(2C)	113(10)
			Zn–N(2)–H(2A)	107(10)
∅Zn	$-NH_3$	207.5	Zn–N(2)–H(2B)	131(10)
∅Zn	$-NH_2$	199.3	Zn–N(2)–H(2C)	100(10)
∅Zn	–N	203.4	H(3A)–N(3)–H(3B)	97(9)
			Zn–N(3)–H(3A)	97(9)
			Zn–N(3)–H(3A)	123(10)
			Zn–N(3)–H(3B)	128(8)
			Zn–N(3)–H(3B)	97(8)
			Zn–N(3)–Zn	116.2(5)

Bromide ions interconnect three $^1_\infty\left[Zn(NH_3)_2(NH_2)_{2/2}^+\right]$ zigzag chains each via eight H-bonds (see Figure 3). Table 7 gives relevant donor–acceptor distances and angles. For both title compounds, there are no indications for a rotational disorder of the ammonia ligands, prohibited by an involvement in hydrogen bonding networks.

Table 7. Donor–acceptor distances (pm) and angles (deg.) in $[Zn_2(NH_3)_2(NH_2)]Br$.

Arrangement	*d*(N–H)	*d*(H . . . Br)	<(NHBr)	*d*(N . . . Br)
N(1)–H(1A) . . . Br	91	280	153.9	364
N(1)–H(1B) . . . Br	89	268	159.2	352
N(1)–H(1C) . . . Br	89	280	146.1	357
N(2)–H(2A) . . . Br	91	268	150.4	351
N(2)–H(2B) . . . Br	89	265	178.6	355
N(2)–H(2C) . . . Br	90	268	173.6	357
N(3)–H(3A) . . . Br	89	283	144.3	360
N(3)–H(3B) . . . Br	89	313	127.4	373

2.2. Raman Spectroscopy

The Raman spectrum (Figure 4) of a $[Zn_2(NH_3)_2(NH_2)_3]Cl$ single crystal can be interpreted according to those of $Zn(NH_3)_2Br_2$ [13], $Zn(NH_3)_6Cl_2$ [14], $[Zn(NH_3)_4]Br_2$ [4], $[Zn(NH_3)_4]I_2$ [4,15] as well as calculations for $[Zn(NH_3)_4]^{2+}$ [16] and is in agreement with general trends for ammoniates of transition metal halides [14,17,18]. Four groups of signals appear in the spectrum, of which three groups are due to modes of NH_3 and NH_2^- molecules (3167–3493 cm^{-1}, 1301–1621 cm^{-1}, 737–1031 cm^{-1}) and one group evokes from Zn–N skeletal vibrations (134–476 cm^{-1}).

In the range of 3167–3493 cm^{-1}, three asymmetric and three symmetric valence vibrations appear in agreement with the three crystallographic different nitrogen sites of ammonia and amide ligands. The broadening of this group of signals indicates the presence of hydrogen bonds of relevant strength, which is in perfect agreement with short NH . . . Cl distances (see above) [18,19]. These hydrogen

bonds are also the reason for a shift to smaller wave numbers as compared to the respective modes of the free ammonia molecule (3337 and 3450 cm^{-1} [20]). For ammoniates of zinc fluoride $Zn(NH_3)_3F_2$ and $Zn(NH_3)_2F_2$ (3093–3337 cm^{-1} [2]), a similar, but even larger shift was observed, due to the higher electronegativity of fluorine compared to chlorine, while the bromide $[Zn(NH_3)_4]Br_2$ (3194 cm^{-1} [4]) and the iodide $[Zn(NH_3)_4]I_2$ (3177 cm^{-1} [21]) exhibit smaller shifts in the symmetric valence mode.

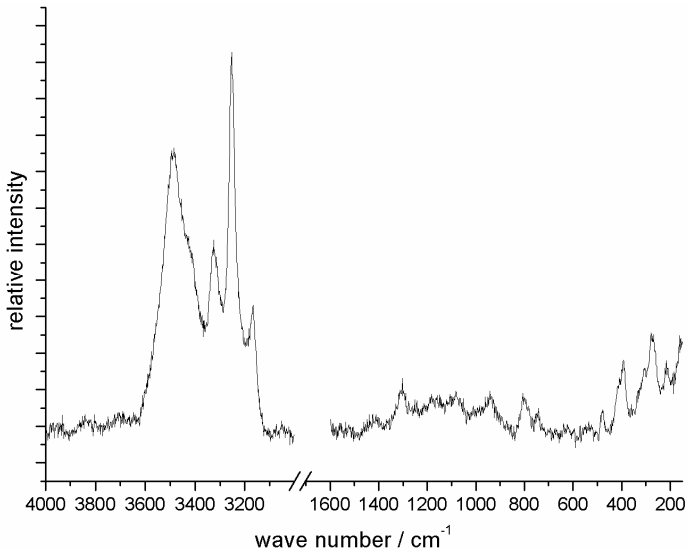

Figure 4. Raman spectrum of $[Zn_2(NH_3)_2(NH_2)_3]Cl$.

The second range is due to the symmetric (1302 cm^{-1}) and asymmetric (1621 cm^{-1}) scissoring modes, which are not resolved for the different crystallographic sites. These vibrations also appear in the spectra of $[Zn(NH_3)_4]Br_2$ (1607 and 1246 cm^{-1} in IR [4]) and $[Zn(NH_3)_4]I_2$ (1615, 1600, 1256 and 1242 cm^{-1} [21]). In comparison to the ammoniates of zinc fluoride, these signals are shifted to lower wave numbers, again as a result of reduced hydrogen bond strength. In the third region (1031–737 cm^{-1}), rocking and wagging modes are present. The rocking vibrations are not present in the spectrum of free ammonia molecules, but are known to increase in intensity with increasing covalent character in complexes [22]. The last range (476–134 cm^{-1}) is due to Zn–N skeleton vibrations.

The absence of signals above 3500 cm^{-1} indicates the absence of significant impurities of OH^- and H_2O, which should provoke a prominent mode at around 3700 cm^{-1} [23].

3. Materials and Methods

3.1. Synthesis

All ammonothermal syntheses were carried out in custom-built autoclaves from austenitic nickel-chromium-based alloy 718 with an inner volume of 97 mL and equipped with a high-pressure valve, a filling line, a rupture disc and a pressure transmitter (HBM P2VA1/5000 bar), which enables continuous pressure monitoring during synthesis [24]. A platinum liner was introduced to minimize contact of the solution with the autoclave wall and thus reduce corrosion. A tubular furnace (LOBA, HTM Reetz GmbH, Berlin, Germany) in vertical position was used to heat the autoclave bodies. Due to unheated installations at the top of the vessel, a natural temperature gradient with a temperature difference of about 100 K developed, resulting in suitable convection for a chemical material transport. Additionally, the applied furnace temperature, which is referred to in the synthesis description, is about 150 K higher than the average reaction temperature [25].

Colorless transparent plate-like crystals $[Zn_2(NH_3)_2(NH_2)_3]Cl$ with maximum size of several hundred µm were obtained from Zn and NH_4Cl (molar ratio 10:1) under ammonothermal conditions (873 K, 97 MPa for 6 h, in 38 h cooling to RT) in the cold zone of the autoclave. In a similar reaction,

$[Zn(NH_3)_2(NH_2)]Br$ was synthesized from Zn and NH_4Br (molar ratio 1:1.7; 773 K, 230 MPa for 12 h, 72 h cooling duration), and colorless crystals were collected from the cold zone. Both compounds are sensitive to moist air and immediately lose their transparency on contact. In the hot zone of the autoclaves, there was always well crystallized $Zn(NH_2)_2$ present along with small amounts of unreacted Zn.

Due to the hygroscopic nature of the reactants and products, all manipulations were carried out inside an argon filled glovebox ($p(O_2) < 0.1$ ppm). A known amount of ammonia was condensed into the autoclave with use of a tensieudiometer [26] for the simultaneous pressure and temperature measurement and a dry ice ethanol cooling bath (T = 198 K). After successful synthesis, the excess ammonia was vented and the autoclave was subsequently evacuated.

3.2. Diffraction Data Collection and Structure Refinements

Selected single crystals were isolated under Ar, sealed in glass capillaries and immediately mounted on a Bruker–Nonius Kappa-CCD diffractometer (Billerica, MA, USA). The chloride was measured at room temperature, while successful intensity data collection on the bromide was only possible if directly cooled to 100 K and subsequently measured (Mo-$K\alpha$ radiation). Structure solution and refinements were carried out using the program package *SHELXL97* [27]. All atom positions except hydrogen were determined by direct methods and anisotropically refined. The hydrogen positions attached to amide groups of the complex amidozincate ions were refined using the riding model, constraining the interatomic N–H distances to 89(2) pm. The isotropic displacement factors U_{iso} were restrained to 1.2/1.5 times the U_{iso} of the nitrogen atom to which they are attached to. For absorption correction, a linear scaling was applied using the absorption correction coefficients 12.93 mm^{-1} ($[Zn_2(NH_3)_2(NH_2)_3]Cl$) and 11.17 mm^{-1} ($[Zn(NH_3)_2(NH_2)]Br$) [28].

$[Zn(NH_3)_2(NH_2)]Br$ suffers from twinning by partial merohedry via a two-fold rotation around [100] in a cell setting in $P112_1/a$. The partial merohedry leads to overlap of reflections (hkl) with $h = 2n$ with those reflections $(h\bar{k}\bar{l})$ of the second twin domain. Reflections with $h = 2n + 1$ are unaffected, but additional reflections $(h\frac{1}{2}kl)$ with $h = 2n + 1$ appear. In the standard setting, $P12_1/n1$, the twinning occurs via a rotation around the face diagonal [101]. Assignment of the reflections to the domains was carried out with the program TWINXLI [29]. Due to application of the twin law, the reliability factors significantly drop from $R_1 = 0.1136$, $wR_2 = 0.227$, GooF = 1.685 (all reflections) to $R_1 = 0.0445$, $wR_2 = 0.0864$, GooF = 1.047 and the residual electron density from $\rho_{max} = 13.29 \times 10^{-6}$ pm^{-3}, $\rho_{min} = -1.51 \times 10^{-6}$ pm^{-3} to $\rho_{max} = 1.23 \times 10^{-6}$ pm^{-3}, $\rho_{min} = -1.13 \times 10^{-6}$ pm^{-3}. Tables A1 and A2 additionally give the final anisotropic displacement parameters. Further details of the crystal structure investigation are available from the Fachinformationszentrum Karlsruhe, 76344 Eggenstein-Leopoldshafen, Germany (Fax: +49-7247-808-666; E-mail: crysdata@fiz-karlsruhe.de, http://www.fiz-karlsruhe.de/request_for_deposited_data.html#c665) on quoting the depository numbers CSD-432188 ($[Zn_2(NH_3)_2(NH_2)_3]Cl$) and CSD-432189 ($[Zn(NH_3)_2(NH_2)]Br$).

3.3. Vibrational Spectroscopy

The solid state Raman spectrum of $[Zn_2(NH_3)_2(NH_2)_3]Cl$ was measured with a Horiba XploRa Raman spectrometer (Kyoto, Japan) coupled with a confocal polarization microscope (Olympus BX51, Tokio, Japan) employing a 638 nm solid state laser at a single crystal sealed in a glass capillary.

4. Conclusions

Zinc metal easily dissolves in ammonia, particularly in ammonoacidic or -basic solutions under ammonothermal conditions. From these solutions at increased temperatures, zinc amide crystallizes. However, quasi-ternary ammoniates of zinc amide halides can also be obtained. With increasing temperatures, condensation of the cationic ions in diamminetriamidodizinc chloride $[Zn_2(NH_3)_2(NH_2)_3]Cl$ and diamminemonoamidozinc bromide $[Zn(NH_3)_2(NH_2)]Br$ occurs via amide ions towards two- and three-dimensional moieties, which can be viewed as sections of the crystal

structure of binary zinc nitride, Zn_3N_2. The formation of amides in solutions containing halide ions, hence nominally ammonoacidic conditions, might be understood by the large excess of Zn, providing an ammonobasic buffer solution $Zn(NH_2)_2/ZnX_2$ in ammonia. Such investigations may pave the way to ammonothermal zinc nitride synthesis and crystal growth, a potential novel nitride semiconductor material for which currently no technique for bulk crystal production is known.

Supplementary Materials: The following are available online at www.mdpi.com/2304-6740/4/4/41/s1.

Acknowledgments: We thank Falk Lissner for collecting the diffraction intensity data. We are much obliged to Werner Massa for providing the program TWINXLI. Furthermore, we thank our cooperation partners of the interdisciplinary research group Ammono-FOR 1600 for the good cooperation and the Deutsche Forschungsgemeinschaft for generous funding.

Author Contributions: Nicolas S. A. Alt and Eberhard Schlücker designed the experimental autoclaves; Theresia M. M. Richter performed the experiments; Theresia M. M. Richter, Sabine Strobel and Rainer Niewa analyzed the data and wrote the paper.

Conflicts of Interest: The authors declare no conflict of interest.

Appendix

Table A1. Anisotropic displacement parameters U_{ij} (10^4 pm^2) for $[Zn_2(NH_3)_2(NH_2)_3]Cl$.

Atom	U_{11}	U_{22}	U_{33}	U_{23}	U_{13}	U_{12}
Zn	0.0195(4)	0.0198(5)	0.0312(5)	−0.0017(4)	0.0006(4)	0.0009(4)
Cl	0.023(1)	0.026(1)	0.025(1)	0	0	0
N(1)	0.014(3)	0.023(3)	0.047(4)	−0.008(4)	0	0
N(2)	0.037(3)	0.039(3)	0.029(3)	0	0.005(3)	0
N(3)	0.022(4)	0.027(5)	0.031(5)	0	0	0

Table A2. Anisotropic displacement parameters U_{ij} (10^4 pm^2) for $[Zn_2(NH_3)_2(NH_2)]Br$.

Atom	U_{11}	U_{22}	U_{33}	U_{23}	U_{13}	U_{12}
Br	0.028(3)	0.0153(4)	0.021(3)	0	−0.003(2)	0
Zn	0.019(3)	0.0126(5)	0.017(3)	0	0	0.002(2)
N(1)	0.03(1)	0.02(1)	0.01(1)	0	0	0
N(2)	0.03(1)	0	0.03(1)	−0.02(1)	0	0
N(3)	0.019(9)	0.011(4)	0.015(9)	0	0	0

References

1. Ehrentraut, D.; Meissner, E.; Bockowski, M. *Technology of Gallium Nitride Crystal Growth*; Springer Materials Sciences: Berlin/Heidelberg, Germany, 2010.
2. Richter, T.M.M.; Le Tonquesse, S.; Alt, N.S.A.; Schlücker, E.; Niewa, R. Trigonal-Bipyramidal Coordination in First Ammoniates of ZnF_2: $ZnF_2(NH_3)_3$ and $ZnF_2(NH_3)_2$. *Inorg. Chem.* **2016**, *55*, 2488–2498. [CrossRef] [PubMed]
3. MacGillavry, C.; Bijvoet, J. The crystal structure of $Zn(NH_3)_2Cl_2$ and $Zn(NH_3)_2Br_2$. *Z. Kristallogr.* **1936**, *94*, 249–255.
4. Eßmann, R. Influence of coordination on N–H···X^- hydrogen bonds. 1. $[Zn(NH_3)_4]Br_2$ and $[Zn(NH_3)_4]I_2$. *J. Mol. Struct.* **1995**, *356*, 201–206. [CrossRef]
5. Kraus, F.; Korber, N. Hydrogen bonds in potassium amide-ammonia(1/2), $KNH_2{\cdot}2NH_3$. *Z. Anorg. Allg. Chem.* **2005**, *631*, 1032–1034. [CrossRef]
6. Zachwieja, U.; Jacobs, H. Tri-μ-amido-bis-[triamminechromium(III)]iodide, $[Cr_2(NH_2)_3(NH_3)_6]I_3$, ein neuer "hexagonaler Perowskit". *Z. Kristallogr.* **1993**, *206*, 247–254.
7. Ketchum, D.; Schimek, G.; Pennington, W.; Kolis, J. Synthesis of new Group III fluoride-ammonia adducts in supercritical ammonia: Structures of $AlF_3(NH_3)_2$ and $InF_2(NH_2)(NH_3)$. *Inorg. Chim. Act.* **1999**, *294*, 200–206. [CrossRef]

8. Jander, J.; Doetsch, V.; Jander, G. *Anorganische und Allgemeine Chemie in Flüssigem Ammoniak*; Akademischer Verlag: Berlin, Germany, 1966.
9. Binnewies, M.; Glaum, R.; Schmidt, M.; Schmidt, P. *Chemical Vapor Transport Reactions*; De Gruyter: Berlin, Germany, 2011.
10. Hertweck, B.; Steigerwald, T.G.; Alt, N.S.A.; Schluecker, E. Different corrosion behaviour of autoclaves made of nickel base alloy 718 in ammonobasic and ammonoacidic environments. *J. Supercrit. Fluids* **2014**, *95*, 158–166. [CrossRef]
11. Juza, R. Amides of the Alkali and the Alkaline earth Metals. *Angew. Chem. Int. Ed.* **1964**, *3*, 471–481. [CrossRef]
12. Liebau, F. *Structural Chemistry of Silicates*; Springer: Berlin, Germany, 1985.
13. Ishikawa, D.N.; Téllez, S.C.A. Infrared and Raman spectra of $Zn(NH_3)_2Br_2$ with ^{15}N and ^{2}H isotopic substitution. *Vibr. Spectrosc.* **1994**, *8*, 87–95. [CrossRef]
14. Nakamoto, K. *Infrared and Raman Spectra of Inorganic and Coordination Compounds*, 4th ed.; Wiley: New York, NY, USA, 1997.
15. Schmidt, K.; Hauswirth, W.; Müller, A. Vibrational Spectra of Nitrogen-15-substituted Hexa-amminenickel(II) Chloride, Hexa-amminecobalt(III) Chloride, and Tetra-amminezinc(II) Iodide. *Dalton Trans.* **1975**, *21*, 2199–2201. [CrossRef]
16. Acevedo, R.; Díaz, G. Normal coordinate analysis for the $M(NH_3)_4^{2+}$ complex ions in D_{4h} and T_d symmetries. Simplified molecular models. *Spectrosc. Lett.* **1986**, *19*, 653–668. [CrossRef]
17. Gauglitz, G.; Vo-Dinh, T. *Handbook of Spectroscopy*; Wiley-VCH: Weinheim, Germany, 2003.
18. Lutz, H.D. Structure and strengt hof hydrogen bonds in inorganic solids. *J. Mol. Struct.* **2003**, *646*, 227–236. [CrossRef]
19. Novak, A. Hydrogen Bonding in Solids. Correlation of Spectroscopic and Crystallographic Data. *Struct. Bond.* **1973**, *18*, 177–216.
20. Svatos, G.F.; Curran, C.; Quagliano, J.V. Infrared Absorption Spectra of Inorganic Coördination Complexes. V. The N–H Stretching Vibration in Coördination compounds. *J. Am. Chem. Soc.* **1955**, *77*, 6159–6163. [CrossRef]
21. Schmidt, K.H.; Müller, A. Vibrational spectra and force constants of pure ammine complexes. *Coord. Chem. Rev.* **1976**, *19*, 41–97. [CrossRef]
22. Mizushima, S.; Svatos, G.F.; Quagliano, J.V.; Curran, C. A Comparison of the Deformation Vibration Frequencies of the Methyl Group With Those of the Coordinated Ammonia Molecule. *Anal. Chem.* **1955**, *27*, 325.
23. Weidlein, J.; Müller, U.; Dehnicke, K. *Schwingungsspektroskopie: Eine Einführung*; Band 2, Thieme: Stuttgart, Germany, 1988.
24. Alt, N.S.A.; Meissner, E.; Schlücker, E.; Frey, L. In situ monitoring technologies for ammonothermal reactors. *Phys. Status Solidi C* **2012**, *9*, 436–439. [CrossRef]
25. Zhang, S. Intermediates during the Formation of GaN under Ammonothermal Conditions. Ph.D. Thesis, University of Stuttgart, Stuttgart, Germany, 2014.
26. Hüttig, G.F. Apparatur zur gleichzeitigen Druck- und Raummessung von Gasen. (Tensi-Eudiometer). *Z. Anorg. Allg. Chem.* **1920**, *114*, 161–173. [CrossRef]
27. Sheldrick, G.M. *SHELXL-97*, Program for the Refinement of Crystal Structure; University of Göttingen: Göttingen, Germany, 1997.
28. Otwinowski, Z.; Minor, W. DENZO and SCALEPACK. In *International Tables for Crystallography F*; Springer: Dordrecht, The Netherlands, 2001; pp. 226–235.
29. Hahn, F.; Massa, W. *TWINXL3.1*, Programm zur Aufbereitung von Datensätzen verzwillingter Kristalle; University of Marburg: Marburg, Germany, 2000.